Мехатроніка і цифрові технології природокористування
Mechatronics and digital technology of nature management

УДК 621.43

Model predictable control of actuator unit with self-tuning feedforward control

Vera Tyrsa[1], Paolo Mercorelli[2], Oleg Sergiyenko[3]

[1]Kharkiv National Technical University of Agriculture, (Kharkiv, Ukraine), vera-tyrsa@mail.ru
[2]Institute of Product and Process Innovation, Leuphana University of Lueneburg, (Lueneburg, Germany), mercorelli@uni.leuphana.de
[3]Instituto de Ingeniería Universidad Autónoma de Baja California, (Mexicali, Baja California, México), srgnk@uabc.edu.mx

This paper describes the use of motor camless engines in hybrid drives. It is known that hybrid drives are composed of piezoelectric and hydraulic parts, as well as switching control model predictable (SCMP). Accounts the effect of hysteresis, and dynamic model Preisach. Control processes in technical systems is often complicated by the presence of hysteresis. The methods set out the submission, are generic and can be applied to a wide variety of processes. In addition, simulations with real data are presented.

Keywords*: hybrid drive, motor camless, switching model, process control, hysteresis, model Preisach.*

I. Introduction.

Camless engine with variation control valve compared with conventional spark ignition engines, has recently attracted a lot of attention. This is caused by its ability to reduce losses in pump operation during partial load and torque productivity increase. To reduce noxious emissions and to increase fuel economy, use the variable valve timing system. This allows you to control the internal EGR. In recent years, guided by the general principles of the use of electromagnetic actuators described in [1] and [2]. The advantages of using a hybrid drive with piezo and hydraulic part is the high precision and the speed of the piezoelectric element and the hydraulic power unit. The expounded management strategy is similar to that which is presented in [3], but this presents a new model of the hydraulic actuator. At the expense quasi absence of inductance effects, with the piezo drive have fewer difficulties with electromagnetic compatibility.

Figure 1 shows the position profiles for the intake and exhaust valves, operating in each cylinder. The graph shows the point of intersection of the trajectory of the intake valve operation during the formation of combustion gases and gasoline. This ensures phase matching with the position of the piston. Fig. 1 also shows the new engine structure with four piezo actuators [4].

The following shows a generalized concept of the operation of individual parts of the engine, for example, control the throttle [5]. This article contains the following sections. Section II describes the proposed model of the drive. Section III is detailed servo piston model and management. Section IV examines the MPC (model predicted control). The conclusions are presented at the end of the simulation.

II. Modeling of a hybrid actuator.

Hysteresis effect affects model-using linearization. In this part of the hysteresis, effect is a model that uses the linearization. We consider the upper and lower bounds of linear characteristics. Figure 2 shows the structure of a hybrid drive. On the left, in the diagram is shown the piezoelectric portion in contact with the piston surface A_1. By a conical structure, the oil-filled, with the piston surface A_1 transmits mechanical movement of the servo piston with a surface A_2. Note that $A_1 >> A_2$ and it implements transmission ratio position of piezo mechanical parts. Therefore, short strokes of the piezo match longer strokes of the mechanical servo. In particular, the ratio

$$W = \frac{A_1}{A_2} \approx 100$$

is multiplied by the position factor of approximately 130, hence the force decreases at the same rate.

Note that the piezo drive, at an elongation at 0 mm produces approximately 30,000 N, and at an elongation of 0.12 mm could create a force of about 10,000 N. Fig. 2 shows four points of the hydraulic circuit (A-B-P-T). Cavities through connecting both pairs of valves (intake and exhaust) are connected to the hydraulic circuit.

After reacting for one piston fuel control valve opens or closes the connecting cavity, and valves are driven by a hydraulic pump through a hydraulic pressure circuit. Details are shown in Fig. 2. T-A connection valve pair connects with the tank, and compound P-B pump. Fig. 2 compound T-A and P-B in open steam valve is closed completely, since the point B is pressurized. Then piezo force increases mechanical servo moves and starts to close the connection. When the mechanical valve actuator is in a middle position, both compounds A-P and B-T are closed and compounds A-P-T and B are opened. In this position, both electrical valves open, so the point A is pressurized. The proposed nonlinear model for the PEA is similar to that shown in [6] and [7]. It consists of a multilayer model (Fig. 3) based on the following hypothesis. According to the proposed sandwich model, the PEA is designed like a three-layer sandwich.

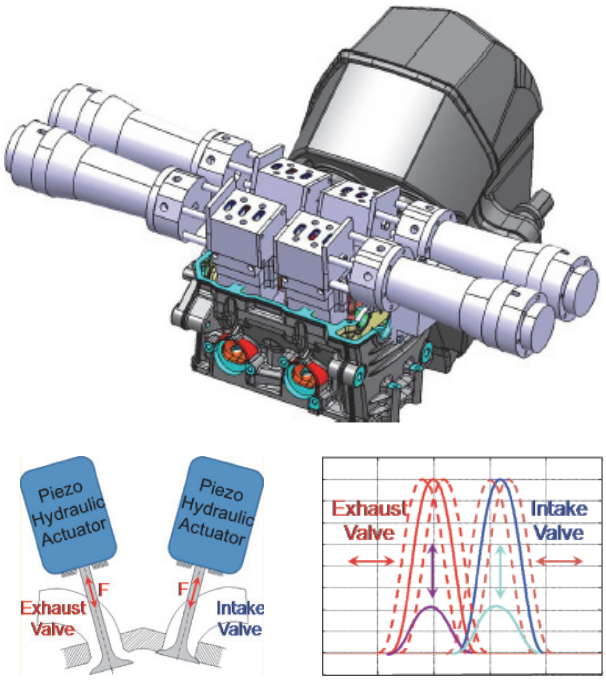

Fig. 1. New structure of the engine. Exhaust and intake piezo hydraulic valve and their opening and closing variable trajectories.

The middle layer is effective piezo layer (P-layer) and the two outer layers are connected to the electrodes. These are known as cooperating layers (I-layer). P-layer has the usual characteristics of the piezoelectric effect, but without the non-linearity hysteresis, so that its behavior is modeled by a linear equivalent circuit. I-layers do not contribute to the appearance of the piezoelectric effect; they are only part of the circuit connecting the P-layer electrode. In [7] it is assumed that each of I-layers may equivalently be represented as a capacitor and a resistor connected in parallel. Together with the equivalent circuit for the P-layer in Fig. 4 is an equivalent circuit for a PEA I-layer non-linearity and hysteresis creep, in which two I-layer joined as C_a and R_a. I-layer capacitor C_a is usually one, he can slightly change some parameters, but here, for simplicity, it will be considered permanent. I-layer resistor R_a is unusual, with significant nonlinearities. Resistance or a fairly large, $R_a > 10^6$ Ω, at a voltage $|| V_a || < V_h$, or a sufficiently small R_a <1000 when $|| V_a || > V_h$. In [7], the threshold voltage V_h, is defined as the hysteresis voltage PEA.

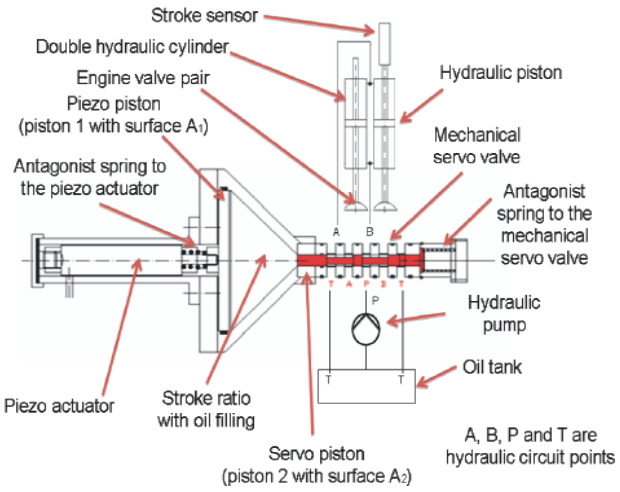

Fig. 2. Scheme of the whole hybrid piezo hydraulic structure

In [7] authors provide a definition of this due with the observation that there is a significant difference and a sharp change in resistance on the threshold voltage, and it is this difference of resistance and therefore the threshold voltage changes in all V_h introduces non-linearity hysteresis and creep PEA. Hysteresis effect may be considered as input function of $V_{in}(t)$ and output $y(t)$ as follows: $H(y(t), V_{in}(t))$, as shown in Fig. 6. According to this model, if $V_h = 0$, the hysteresis disappears and if $R_a = \infty$, where $|| V_a || < V_h$, the creep will also disappear. Based on the proposed model and the equivalent circuit of the sandwich, as shown in Fig. 4, we can receive additional health model as follows:

$$\dot{V}_a(t) = -\left(\frac{1}{R_a} + \frac{1}{R_0}\right)\frac{V_a(t)}{C_a} - \frac{V_z(t)}{C_a R_o} + \frac{V_{in}(t)}{C_a R_o}, \quad (1)$$

$$\dot{V}_z(t) = \frac{\dot{Q}_b}{C_z} + \frac{1}{C_z}\left(-\frac{V_a(t)}{R_0} - \frac{V_z(t)}{R_0} + \frac{V_{in}(t)}{R_0}\right). \quad (2)$$

© В.В. Тырса, П. Меркорелли, О.Ю. Сергиенко, 2017
© V.V. Tyrsa, P. Mercorelli, O.Yu. Sergiyenko, 2017

Where $Q_b = D_y F_z(t)$ is the "backward electric charge power" (back-EMF) in the PEA, [7].

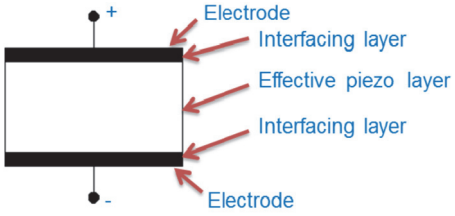

Fig. 3. The sandwich model of the PEA

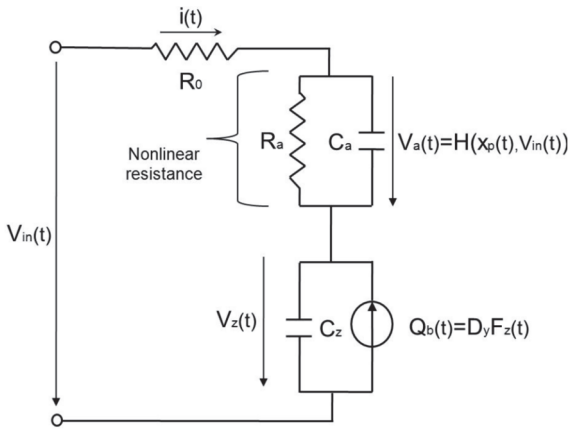

Fig. 4. Electrical part of the model

According to [7] in the notation in Fig. 5, we can write:

$$F_z(t) = \frac{M_p}{3}\ddot{x}(t) + D\dot{x}(t) + Kx(t) + K_x x(t). \quad (3)$$

K and D – the elasticity and spring of constant friction, which is an antagonist of the piezoelectric effect. C_z – total capacity of the PEA, R_0 – contact resistance. More details on this model are presented in [7]. Considering the system shown in Fig. 2 as a whole, assuming that the oil is not compressed, the entire mechanical system represented in elastic mass structure is shown in Fig. 5.

The following notation is used in this system: K_x is a constant factor of PEA elasticity. In the technical literature the factor $D_x K_x = T_{em}$ is known as the transformation ratio and is the most important characteristic of the electromechanical transducer. $M_p/3$ – in this case, the moving mass of the piezo structure, which is part of the entire mass of the piezo, the MSK – the mass of the piston and the amount of oil moving actuator, the valve M_v weight. It may be noted that the moving mass of the piezo structure is only part of the whole piezo mass. The value of this part of the obtained piezoelectric device manufacturers and is determined by experimental measurements. KSK and DSK spring characteristics antagonist mechanical servo valve, see. Fig. 2. D_{oil} friction oil constant. Furthermore, according to [7], the movement $x_p(t)$ in the diagram Fig. 5.

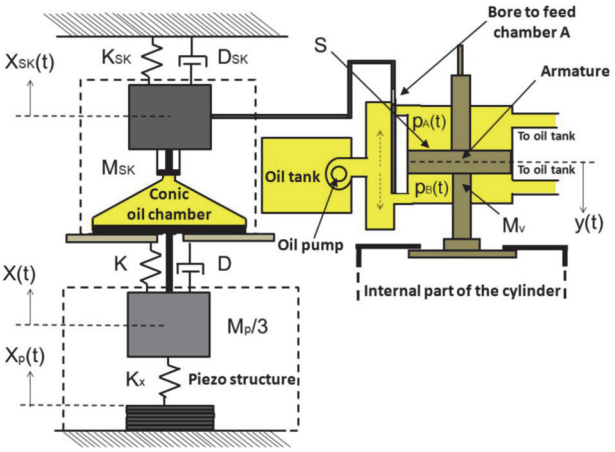

Fig. 5. Scheme of the whole actuator

$$x_p(t) = D_x V_x(t). \quad (4)$$

According to the scheme in Fig. 4 can be written as follows:

$$V_z = V_{in}(t) - R_0 i(t) - H(x_p(t), V_{in}(t) \quad (5)$$

where R_0 of connection resistance and the $i(t)$ is the input current, as shown in Fig. 4. As the function describing the effect of the hysteresis mentioned above, and as shown in simulation in Fig. 6 is taken into account $H(x_p(t), V_{in}(t))$. Taking into account all the system described in Fig. 2, electrical and mechanical system described in Fig. 4, 5 and 6 may be represented by the following mathematical expression:

$$\frac{M_p}{3}\ddot{x}(t) + M_{SK}\ddot{x}_{SK}(t) + Kx(t) + D\dot{x}(t) + \\ + K_{SK}x_{SK}(t) + D_{SK}\dot{x}_{SK}(t) + D_{oil}\dot{x}_{SK}(t) + \\ + K_x\left(x(t) - \Delta x_p\left(V_{in}(t)\right)\right) = 0, \quad (6)$$

where $\Delta x_p(t)$ is a function of the interval $x_p(t)$, as shown in Fig. 6 which, in accordance with the equation (4) may be expressed as:

$$\Delta x_p(t) = D_x \Delta V_z(t). \quad (7)$$

Using equations (5) and (7), we obtain the following equation:

$$K_x \Delta x_p(t) = K_x D_x\left(V_{in}(t) - H\left(\Delta x_p(t), V_{in}(t)\right)\right), \quad (8)$$

Which represents the spacing force generated by the piezoelectric device. Equation (6) can be expressed as follows:

$$\frac{M_p}{3}\ddot{x}(t) + M_{SK}\ddot{x}_{SK}(t) + Kx(t) + \\ + D\dot{x}(t) + K_{SK}x_{SK}(t) + D_{SK}\dot{x}_{SK}(t) + \\ + D_{oil}\dot{x}_{SK}(t) + K_x x(t) = K_x \Delta x_p\left(V_{in}(t)\right). \quad (9)$$

It should be noted that the relation in stationary or quasi-static dynamic conditions is:

$$x_{SK}(t) \approx Wx(t), \quad (10)$$

where W ratio above a certain position, which takes into account the incompressibility of the oil in a conical chamber. $F_d(t)$ opposite the combustion pressure relative strength.

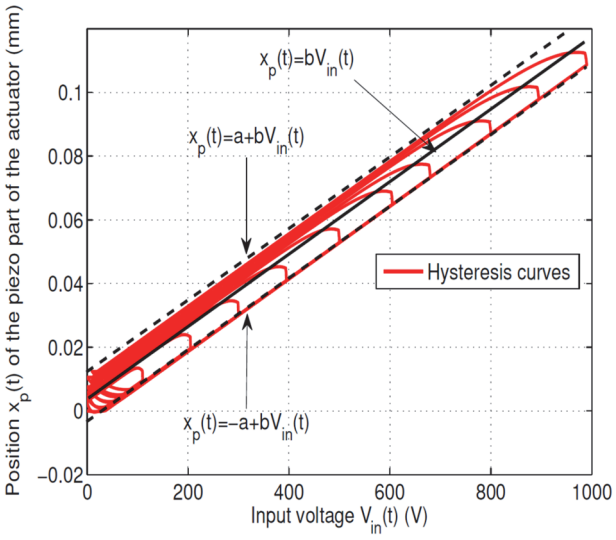

Fig. 6. Simulated hysteresis curve of the piezo part of the actuator: $H(x_p(t), V_{in}(t))$

III. Performance robust model system of predicting control

Using grid affine linear functions can be described by the hysteresis phenomenon. Fig. 6 clearly indicates the upper and lower bounds of the grid. Using Affine linear functions can be written:

$$\Delta x_p\big(V_{in}(t)\big) = [-a\ a] + bV_{in}(t), \quad (11)$$

Where a ∈ R and b ∈ R – these are positive constants. In particular:

$$\underline{\Delta} x_p\big(V_{in}(t)\big) = -a + bV_{in}(t), \quad (12)$$

and

$$\overline{\Delta} x_p\big(V_{in}(t)\big) = a + bV_{in}(t). \quad (13)$$

With these designations, the system presented in (6) can be divided into two subsystems:

$$\frac{M_p}{3}\ddot{x}(t) + M_{SK}\ddot{x}_{SK}(t) + Kx(t) + D\dot{x}(t) + K_{SK}x_{SK}(t) + D_{SK}\dot{x}_{SK}(t) + D_{oil}\dot{x}_{SK}(t) + K_x x(t) = K_x \underline{\Delta} x_p\big(V_{in}(t)\big), \quad (14)$$

and

$$\frac{M_p}{3}\ddot{x}(t) + M_{SK}\ddot{x}_{SK}(t) + Kx(t) + D\dot{x}(t) + K_{SK}x_{SK}(t) + D_{SK}\dot{x}_{SK}(t) + D_{oil}\dot{x}_{SK}(t) + K_x x(t) = K_x \overline{\Delta} x_p\big(V_{in}(t)\big), \quad (15)$$

where

$$\underline{\Delta} x_p\big(V_{in}(t)\big) = -a + bV_{in}(t) \text{ and } \overline{\Delta} x_p\big(V_{in}(t)\big) = a + bV_{in}(t).$$

A. The structure of the pre-emptive self-tuning

The inversion model is considered only in the mechanical part. In accordance with the real data, piezoelectric and hydraulic modeling of the results is by more than 10 times faster than mechanical. In view of the above, confirmed a posteriori modeling, the predictive controller is digitized by the equation:

$$u_{fed}(t) = \frac{\left(\frac{M_p}{3} + M_{SK}W\right)\ddot{y}_d(t)}{K_x b} + \frac{(D + (D_{SK} + D_{oil})W)\dot{y}_d(t)}{K_x b} + \frac{(K + K_x + K_{SK})y_d(t) + K_x(-1)^q a}{K_x b} + u_0, \quad (16)$$

where $y_d(t)$ is the desired position trajectory valve and q – is the parameter of the switching so that q = 1, 2. It should be noted that the voltage u0 is a voltage that allows moving the piezo-actuator to a position in which the mechanical control valve is located in the middle of the oil chamber, so that the pressure in the valve is zero. The point of equilibrium is achieved in such conditions, and the valve is controlled. MPC allows you to design the structure of pre-emptive self-tuning in a more reliable way.

B. The hydraulic drive part

Fig. 7 shows a possible linear model used in practice. This model is described in [8], its possible linear approximation is used in industry, especially in industrial buildings represented in [8]. Figure 7 presents a model in which we can see the following options: T_H – time constant of the hydraulic part, T_M – time constant of the mechanical part. V_H and V_M – are in a steady state transfer function hydromechanical factors. Another parameter that characterizes the hydraulic mechanical model is *K2Lidx*. In reality, the *K2Lidx* parameter is a characteristic speed value that depends on the internal leakage. This parameter is multiplied by the speed of the valve and releases the mass flow, as shown in the flowchart (Fig. 7).

Parameter A_{AK} – the surface of the moving parts (servo). From Fig. 7 and taking into account that the variable Q_{th} is the mass flow in the hydraulic actuator, obtain the following:

$$b_m = Q_{th}(s) - a_m\,, \quad (17)$$

$$V_V(s) = b_m \cdot \frac{V_H \cdot V_M \cdot A_{AK}}{(T_H \cdot s + 1)(T_M \cdot s + 1)}, \quad (18)$$

$$V_V(s) = b_m \cdot \frac{V_H \cdot V_M \cdot A_{AK}}{T_H \cdot T_M \cdot s^2 + (T_H + T_M) \cdot s + 1}, \quad (19)$$

© В.В. Тырса, П. Меркорелли, О.Ю. Сергиенко, 2017
© V.V. Tyrsa, P. Mercorelli, O.Yu. Sergiyenko, 2017

$$a_m = V_{V(s)} \cdot (A_{AK} + K2Lidx), \quad (20)$$

$$b_m = Q_{th}(s) - V_V(s) \cdot (A_{AK} + K2Lidx), \quad (21)$$

$$V_V(s) = \big(Q_{th}(s) - V_V(s) \cdot (A_{AK} + K2Lidx)\big) \times \times \cdot \frac{V_H \cdot V_M \cdot A_{AK}}{T_H \cdot T_M \cdot s^2 + (T_H + T_M) \cdot s + 1}. \quad (22)$$

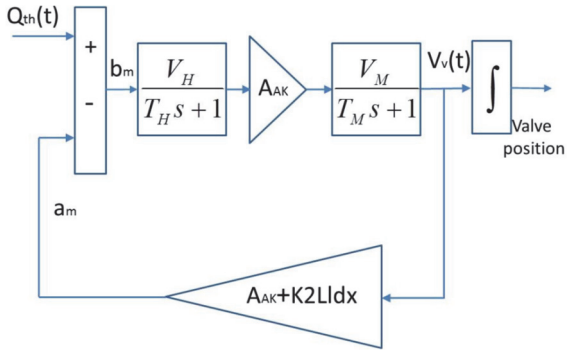

Fig. 7. Hydraulic model structure

Given the transfer function:

$$\frac{V_V(s)}{Q_{th}(s)} = \frac{d_m}{a_m \cdot s^2 + b_m \cdot s + c_m}, \quad (23)$$

where:

$$a_m = T_H \cdot T_M, \quad (24)$$

$$b_m = T_H + T_M, \quad (25)$$

$$c_m = 1 + V_H \cdot V_M \cdot A_{AK} \cdot (A_{AK} + K2Lidx), \quad (26)$$

$$d_m = V_H \cdot V_M \cdot A_{AK}, \quad (27)$$

$$a_m \cdot s^2 \cdot V_V(s) + b_m \cdot s \cdot V_V(s) + + c_m \cdot V_V(s) - d_m \cdot Q_{th}(s) = 0. \quad (28)$$

Given the inverse Laplace transform:

$$a_m \cdot \ddot{V}_V(t) + b_m \cdot \dot{V}_V(t) + c_m \cdot V_V(t) - -d_m \cdot Q_{th}(t) = 0. \quad (29)$$

Looking at the following positions:

$$x_1(t) = V_V(t), \quad (30)$$

$$x_2(t) = \dot{x}_1(t), \quad (31)$$

then:

$$\dot{x}_1(t) = x_2(t), \quad (32)$$

$$\dot{x}_2(t) = \frac{1}{a_m} \times \times \big(d_m Q_{th}(t) - b_m x_2(t) - c_m x_1(t)\big), \quad (33)$$

and

$$\begin{bmatrix} \dot{x}_1(t) \\ \dot{x}_2(t) \end{bmatrix} = \begin{bmatrix} 0 & 1 \\ -\frac{c_m}{a_m} & -\frac{b_m}{a_m} \end{bmatrix} \cdot \begin{bmatrix} x_1(t) \\ x_2(t) \end{bmatrix} + + \begin{bmatrix} 0 \\ \frac{b_m}{a_m} \end{bmatrix} \cdot Q_{th}(t). \quad (34)$$

If the position of the valve *y(t)* is considered, then the following system should be considered:

$$\begin{bmatrix} \dot{y}(t) \\ \dot{x}_1(t) \\ \dot{x}_2(t) \end{bmatrix} = \begin{bmatrix} 0 & 1 & 0 \\ 0 & 0 & 1 \\ 0 & -\frac{c_m}{a_m} & -\frac{b_m}{a_m} \end{bmatrix} \cdot \begin{bmatrix} y(t) \\ x_1(t) \\ x_2(t) \end{bmatrix} + + \begin{bmatrix} 0 \\ 0 \\ \frac{d_m}{a_m} \end{bmatrix} \cdot Q_{th}(t). \quad (35)$$

Variable $Q_{th}(t)$ – the volume flow, which is a linear function of the pressure and the position of the servo piston. Given that between the position of the servo piston and the piezo in a quasi-static state of the following is true:

$$x_{SK}(t) \approx Wx(t),$$

the total ratio between and Q_{th} *x (t)* as follows:

$$Q_{th}(t) = \big(\sqrt{p_0 - p_T} - \sqrt{p_T}\big) Cost. \times \times \sqrt{\frac{2}{p_l}} Wx(t), \quad (36)$$

where "Cost" is a constant depending on the size of the slots, for more details see [8].

IV. Robust reporting system and switch model predicting control.

As is evident from Fig. 6, which shows the upper and lower boundaries of the hysteresis curve can be written as follows:

$$\Delta x_p\big(V_{in}(t)\big) = [-a\ a] + bV_{in}(t), \quad (37)$$

Where a ∈ R and b ∈ R are positive constants. In particular,

$$\underline{\Delta} x_p\big(V_{in}(t)\big) = -a + bV_{in}(t) \quad (38)$$

and

$$\overline{\Delta} x_p\big(V_{in}(t)\big) = a + bV_{in}(t). \quad (39)$$

Given these notations presented in (6) can be divided into the following two systems:

$$\frac{M_p}{3} \ddot{x}(t) + M_{SK} \ddot{x}_{SK}(t) + Kx(t) + + D\dot{x}(t) + K_{SK} x_{SK}(t) + D_{SK} \dot{x}_{SK}(t) + + D_{oil} \dot{x}_{SK}(t) + K_x x(t) = \underline{\Delta} x_p\big(V_{in}(t)\big), \quad (40)$$

$$\frac{M_p}{3} \ddot{x}(t) + M_{SK} \ddot{x}_{SK}(t) + Kx(t) + + D\dot{x}(t) + K_{SK} x_{SK}(t) + D_{SK} \dot{x}_{SK}(t) + + D_{oil} \dot{x}_{SK}(t) + K_x x(t) = \overline{\Delta} x_p\big(V_{in}(t)\big). \quad (41)$$

Assume the system state variables are the following:

$$x(t) = [x_{1p}(t)\ x_{2p}(t)\ x_{0h}(t)\ x_{1h}(t)\ x_{2h}]^T, \quad (42)$$

where $x_{1p}(t)=x(t)$, $x_{2p}(t)=\dot{x}(t)$ are speed positions and piezo respectively. $x_{0h}(t) = y(t)$, $x_{1h}(t) = \dot{x}_1(t)$ and $x_{2h}(t) = \dot{x}_2(t)$ represent the position, speed and acceleration of the hydraulic valve. The selected model can be rewritten as follows:

$$x(k+1) = x(k) + + T_s\big(A_k x(k) + B_k u(k) + E_k d(k)\big), \quad (43)$$

where T_s – sampling time with parameter $k = 1, 2, ... N$. In view of equation (35) and (39) and (38) in combination with (40) and (41), we obtain the following matrix representation for the system:

$$A_k = \begin{bmatrix} 0 & 1 & 0 & 0 & 0 \\ A_{21} & A_{22} & 0 & 0 & 0 \\ 0 & 0 & 0 & 1 & 0 \\ 0 & 0 & 0 & 0 & 1 \\ A_{51} & 0 & 0 & A_{54} & A_{55} \end{bmatrix}, \quad (44)$$

где:

$$A_{21} = -\frac{(K_x + K + K_{SK}W)}{\frac{M_p}{3} + M_{SK}W};$$

$$A_{22} = \frac{(D + (D_{SK} + D_{oil})W)}{\frac{M_p}{3} + M_{SK}W};$$

$$A_{52} = \frac{D_m W}{a_m};\ A_{54} = -\frac{c_m}{a_m};\ A_{55} = -\frac{b_m}{a_m}.$$

$$E_k = \begin{bmatrix} 0 & 0 & 0 & 0 & 0 \\ 0 & E_{22} & 0 & 0 & 0 \\ 0 & 0 & 0 & 0 & 0 \\ 0 & 0 & 0 & 0 & 0 \\ 0 & 0 & 0 & 0 & E_{55} \end{bmatrix}, \quad (45)$$

где:

$$E_{22} = \frac{3K_x a}{M_p + 3M_{SK}W};\quad E_{55} = -\frac{1}{M_v}.$$

$$B_k = \begin{bmatrix} 0 \\ \frac{3K_x a}{M_p + 3M_{SK}W} \\ 0 \\ 0 \\ 0 \end{bmatrix} \quad d(k) = \begin{bmatrix} 0 \\ T_r(k) \\ 0 \\ 0 \\ -F_L(K) \end{bmatrix} \quad (46)$$

where the term $F_L(t)$ is an disturbance. As a rule, this disturbance is present in the exhaust valve due to the presence of internal pressure after combustion.

$$T_r = -sign\big(V_{in}(k) - V_{in}(k-1) - V_h(k)\big), \quad (47)$$

where $V_h(k)$ is the appropriate threshold voltage, as proposed for the construction of the hysteresis in [7]. The term T_r shows the switching character of the model.

A. Solution of optimization problems in the linear position of MPC

Considering model described in the MPC that the standard sampling Euler considered with $k = nT_s$, $n \in N$, where T_s – sampling time, if $y(t)$ is supposed to control output, we get:

$$\begin{aligned} x(k+1) &= A_k x(k) + B_k V_{in}(k) + E_k d(k), \\ y(k) &= H_k x(k), \end{aligned} \quad (48)$$

where the matrix H_k = [0 0 1 0 0] is the output matrix, which determines the position of the valve. The matrix A_k is a digitizing system described in (44). Particular attention should be paid to the matrix B_k, E_k and d_k, taking into account the switching aspect of the present system. The MPC method considers only two models.

$$\begin{aligned} \hat{y}(k+1) &= H_k A_k x(k) + \\ &+ H_k B_k u_{mpc}(k) + H_k E_k d(k), \end{aligned} \quad (49)$$

$$\begin{aligned} \hat{y}(k+2) &= H_k {A_k}^2 x(k) + H_k A_k B_k u_{mpc}(k) + \\ &+ H_k B_k u_{mpc}(k+1) + H_k A_k E_k d(k) + \\ &+ H_k E_k d(k). \end{aligned} \quad (50)$$

Equations (49) and (50) can be expressed vectorially as follows:

$$Y(k) = G_p x(k) + F_{1p}(k) U_{mpc}(k) + F_{2p} d(k). \quad (51)$$

If the following criterion of effectiveness suggest

$$\begin{aligned} J = \frac{1}{2}\sum_{j=1}^{N} \big(y_d(k+j) - \hat{y}(k+j)\big)^T \times \\ \times Q_p\big(y_d(k+j)) - \hat{y}(k+j)\big) + \\ + \frac{1}{2}\sum_{j=1}^{N-1} \Big(u_{mpc}(\,k+\,j)\Big)^T R_p u_{mpc}(k+j)), \end{aligned} \quad (52)$$

where $y_d(k + j)$, $j = 1, 2, . . .,N$ is the initial position of the trajectory (desired trajectory) and N is the number of samples and the forecasting horizon R_p and Q_p certain non-negative matrix, the index performance solutions to minimize (52) can then be obtained by solving

$$\frac{\partial J}{\partial u_{mpc}} = 0. \quad (53)$$

If we consider only two steps up to the forecast horizon, then:

$$F_{1p} = \begin{bmatrix} H_k & 0 \\ H_k(A_k B_k + B_k) & H_k B_k \end{bmatrix}, \quad (54)$$

$$G_p = \begin{bmatrix} H_k & A_k \\ H_k & {A_k}^2 \end{bmatrix} \quad (55)$$

and

$$F_{2p} = \begin{bmatrix} H_k E_k & 0 \\ H_k(A_k E_k + E_k) & H_k E_k \end{bmatrix}. \quad (56)$$

A direct calculation can be obtained offline explicitly:

$$\begin{aligned} u_{mpc}(k) &= u_{mpc}(k-1) + \\ &+ \big(F_{1p}^T Q_p F_{1p} + R_p\big)^{-1} \times \\ &\times \left(F_{1p}^T Q_p \left(Y_{d_p}(k) - G_p x(k) - F_{2p} d(k)\right)\right). \end{aligned} \quad (53)$$

Where $Y_{dp}(k)$ and $Y_p(k)$ are the output column vector of the desired and measured or monitored output vector. For details, see [9].

V. Simulation

Fig. 8 shows the simulated results of the final track position control valve and an exhaust valve speed. These paths correspond to 8000 revolutions per minute (RPM). The received power for each exhaust valve has a maximum value of 1 kW, and its average value does not exceed 300 watts at 8000 rpm. In this case, the maximum current is 1.5 Ampere, with simulated pressure. Simulated

© В.В. Тырса, П. Меркорелли, О.Ю. Сергиенко, 2017
© V.V. Tyrsa, P. Mercorelli, O.Yu. Sergiyenko, 2017

pressure acts on the valve, prepared as a function of the exponent of the valve position. Modeling influences horizon, consisting of two samples. The digital controller is configured to work with a sampling time of 20×10^{-6} *sec* in accordance with the specifications of a digital signal processor, in which we intend to test the system.

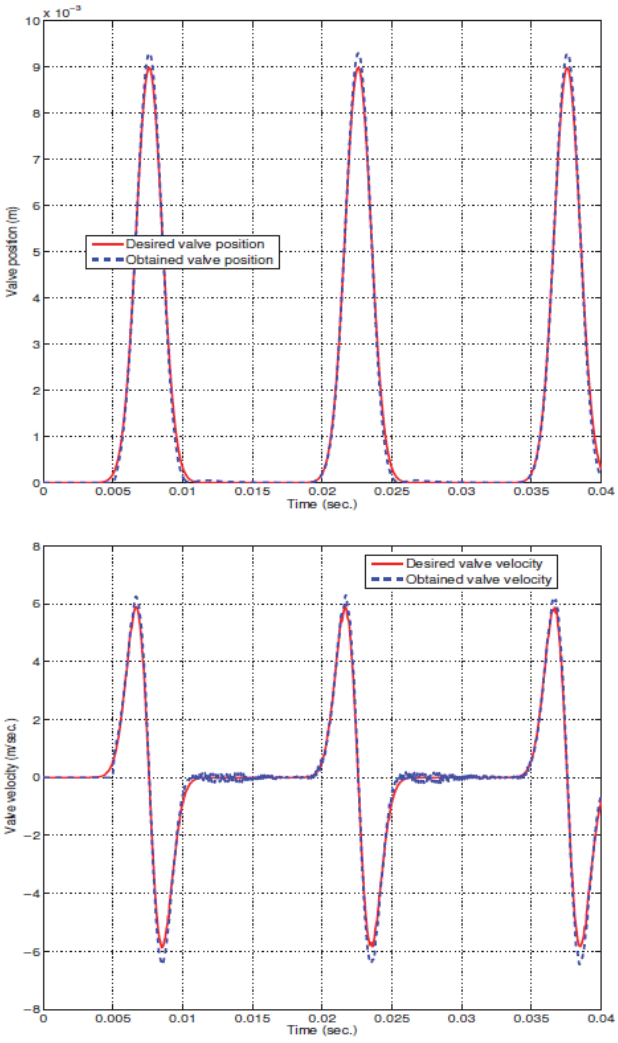

Fig. 8. Simulated results (8000 rpm). On the top: Desired and obtained position. On the bottom: Desired and obtained valve velocity

VI. Conclusion

The article deals with a hybrid drive consisting of piezoelectric and hydraulic parts containing the structure switching control model predicted (SCMP) for the engine. In this paper, we take into account the dynamic model Preisach hysteresis. In addition, simulations with real data are presented.

References

1. P. Mercorelli. A two-stage augmented extended Kalman filter as anvobserver for sensorless valve control in camless internal combustionvengines. *IEEE Transactions on Industrial Electronics*, 59(11): 4236 - 4247, 2012.

2. P. Mercorelli. A hysteresis hybrid extended Kalman filter as an observer for sensorless valve control in camless internal combustion engines. *IEEE Transactions on Industry Applications*, 48(6): 1940 - 1949, 2012.

3. P. Mercorelli. A switching Kalman filter for sensorless control of a hybrid hydraulic piezo actuator using MPC for camless internal combustion engines. In *Proceedings of IEEE International Conference on Control Applications (CCA)*, 2012.

4. P. Mercorelli and N. Werner. A hybrid actuator modelling and hysteresis effect identification in camless internal combustion engines control. *International Journal of Modelling, Identification and Control*, 21(3): 253 - 263, 2014.

5. P. Mercorelli. Robust feedback linearization using an adaptive PD regulator for a sensorless control of a throttle valve. *Mechatronics a journal of IFAC. Elsevier publishing*, 19(8): 1334 - 1345, 2009.

6. H.J.M.T.A. Adriaens, W. L. de Koning, and R. Banning. Modeling piezoelectric actuators. *IEEE / ASME Transactions on Mechatronics*, 5(4): 331 - 341, 2000.

7. Y.-C. Yu and M.-K. Lee. A dynamic nonlinearity model for a piezoactuated positioning system. In *Proceedings of the 2005 IEEE International Conference on Mechatronics*, 2005.

8. H. Murrenhoff. *Servohydraulik*. Shaker Verlag, Aachen, 2002.

9. H. Sunan, T.K. Kiong, and L.T. Heng. *Applied Predictive Control*.Springer-Verlag London, Printed in Great Britain, 2002.

Аннотация

Модель прогнозируемого управления исполнительным механизмом с возможностью самонастройки

В.В. Тырса, П. Меркорелли, О.Ю. Сергиенко

В статье описано применение моторных безкулачковых двигателей в гибридных приводах. Гибридные приводы состоят из пьезоэлектрической и гидравлической частей, а также коммутационной модели прогнозируемого контроля (КМПК). Учитывается влияние гистерезиса и динамическая модель Прейзаха. Контроль процессов, происходящих в технических системах часто

осложняется наличием гистерезиса. Методы, изложенные в представленном материале, носят обобщенный характер и могут применяться для самых разнообразных процессов. Также представлено моделирование с реальными данными.

Ключевые слова*: гибридный привод, безкулачковый двигатель, коммутационная модель, контроль процессов, гистерезис,* модель Прейзаха.

Анотація

Модель прогнозованого управління виконавчим механізмом з можливістю самоналаштування

В.В. Тирса, П. Меркореллі, О.Ю. Сергієнко

У статті описано застосування моторних безкулачкових двигунів в гібридних приводах. Гібридні приводи складаються з п'єзоелектричної і гідравлічної частин, а також комутаційної моделі прогнозованого контролю (КМПК). Враховується вплив гістерезису і динамічна модель Прейзаха. Контроль процесів, що відбуваються в технічних системах часто ускладняється наявністю гістерезису. Методи, викладені в представленому матеріалі, носять узагальнений характер і можуть застосовуватися для найрізноманітніших процесів. Також представлено моделювання з реальними даними.

Ключові слова*: гібридний привід, безкулачковий двигун, комутаційна модель, контроль процесів, гістерезис, модель Прейзаха.*

Представлено від редакції: А.Т. Лебедєв / Presented on editorial: A.T. Lebedjev
Рецензент: Р.В. Антощенков / Reviewer: R.V. Antoshhenkov
Подано до редакції / Received: 25.07.2016

© В.В. Тырса, П. Меркорелли, О.Ю. Сергиенко, 2017
© V.V. Tyrsa, P. Mercorelli, O.Yu. Sergiyenko, 2017